# Time-dependent modelling of 104/137 GHz X2-mode ECRH on ST40 to aid future scenario development

*Nicolas* Lopez*, *Xin* Zhang, *Michele* Romanelli, *Aleksandra* Alieva, *Vladimir* Shevchenko, and ST40 Team

Tokamak Energy Ltd, Milton, Abingdon, United Kingdom

**Abstract.** With a multi-Tesla magnetic field and the capability to achieve fusion-relevant ion temperatures, the ST40 experiment is uniquely positioned as a high-performance spherical tokamak on which to test reactor-relevant technologies. This will be further augmented by the addition of a 104/137 GHz dual-frequency gyrotron supplied by Kyoto Fusioneering Ltd capable of delivering 2s pulses of 1 MW EC power. Here we demonstrate the new capabilities afforded by the additional ECRH through time-dependent integrated modelling in TRANSP. Using two different reference shots, we find that, although accessibility constraints make it difficult to directly drive EC current, the 1MW 104 GHz X2-mode ECRH is nevertheless capable of reducing the loop voltage by increasing the bootstrap current via direct electron heating. The safety-factor profile is also strongly modified, attaining reverse shear in one scenario. More flexibility in the EC launcher geometry will be gained by increasing the magnetic field from 1.8 to 2.4 T; in this case, X2-mode ECRH at 137 GHz could be used instead, which will not suffer any accessibility constraints at typical ST40 densities.

## 1 Introduction

Although EC-only startup, rampup, and sustainment scenarios are being increasingly suggested for fusion pilot plants due to the immense operational benefits they would offer [1, 2], there is also broad consensus that such techniques must be experimentally validated as soon as possible to conform with the ambitious timelines of these projects. Looking towards these goals, a 104/137 GHz, 1 MW gyrotron is currently being installed on the ST40 spherical tokamak [3] located at Tokamak Energy Ltd in Oxfordshire, UK. Preliminary modeling using standalone ray-tracing on simple analytical plasma profiles [4] suggests that second-harmonic X-mode (X2-mode) heating and current drive can be effectively performed over a reasonable range of parameters.

However, it has been shown previously [5] that including the time-dependent plasma response to the EC absorption is crucial to accurately assess the EC performance. Therefore, in this work we perform time-dependent integrated modeling of 104/137 GHz X2-mode ECRH on ST40 using the transport code TRANSP [6]. This modeling is done using experimental shots as reference, allowing for more realistic assessment of refraction effects on the wave propagation than analytic profiles would allow. Also, the original ST40 EC modeling [4] was performed assuming ST40 could achieve its nominal full field of 3 Tesla. To date, 1-2 Tesla fields are more typically achieved. Therefore it is of interest to repeat the modeling using experimentally obtained magnetic equilibria to determine whether increasing the ST40 magnetic field is necessary for the upcoming EC experimental campaign.

*Corresponding author: nicolas.lopez@tokamakenergy.com

## 2 ST40 parameter summary

ST40 [3] is a spherical tokamak whose geometric center $R_0$ is around 40-50 cm with an aspect ratio that can vary between 1.6 and 1.9. To date, the magnetic field strength at $R = 40$ cm has varied over the range 0.9-2.1 T with typical value of 1.8 T, although it is planned to increase the field strength to 2.4 T for the upcoming EC campaign. The low aspect ratio of ST40 implies that the magnetic field magnitude varies by a factor of 4 over the plasma volume, as shown in Fig. 1. Plasma currents ranging from 0.25-0.8 MA can be generated using a combination of merging-compression (MC) startup and two neutral beams (NB) with combined power of 1.8 MW. The MC startup implies that there is no current rampup phase, as the plasma is initialized at nearly full current; the central solenoid then sustains the plasma current for flattop times $\lesssim 180$ ms.

For typical ST40 parameters of $T_e \sim 1$ keV and $n_e \sim 6 \times 10^{19}$ m$^{-3}$, the X2-mode is expected to be absorbed (Fig. 1) at both 104 and 137 GHz, provided the magnetic field strength is set to place the absorption near the plasma core. Both resonant frequencies will be accessible as well (Fig. 2), although 104 GHz is only marginal. Here, the X2 absorption is estimated using the optical thickness for perpendicular propagation [7] for simplicity:

$$\tau_{X2} = \frac{\pi T \omega R_0}{mc^3} \frac{\alpha(6-\alpha)^{5/2}\sqrt{2-\alpha}}{16(3-\alpha)^{5/2}}, \quad \alpha = \frac{4\omega_p^2}{\omega^2}. \tag{1}$$

In subsequent sections, $\tau_{X2}$ will be computed self-consistently with the X2 ray trajectory via ray-tracing.

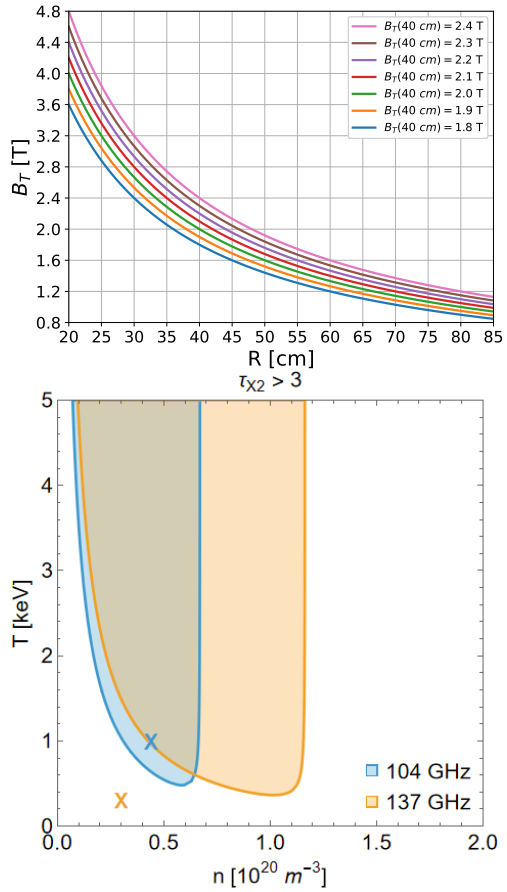


**Figure 1.** (Top) Simple $1/R$ variation of B along midplane over the range of $R$ within ST40, with values of $B$(40cm) ranging from 1.8 to 2.4 T in steps of 0.1 T. (Bottom) Region of strong X2 absorption at 104 and 137 GHz, using Eq. (1) for $\tau_{X2} > 3$. The colored X's mark the plasma parameters that occur when the EC ray crosses the X2 resonance in Fig. 3 (blue) and Fig. 4 (orange).

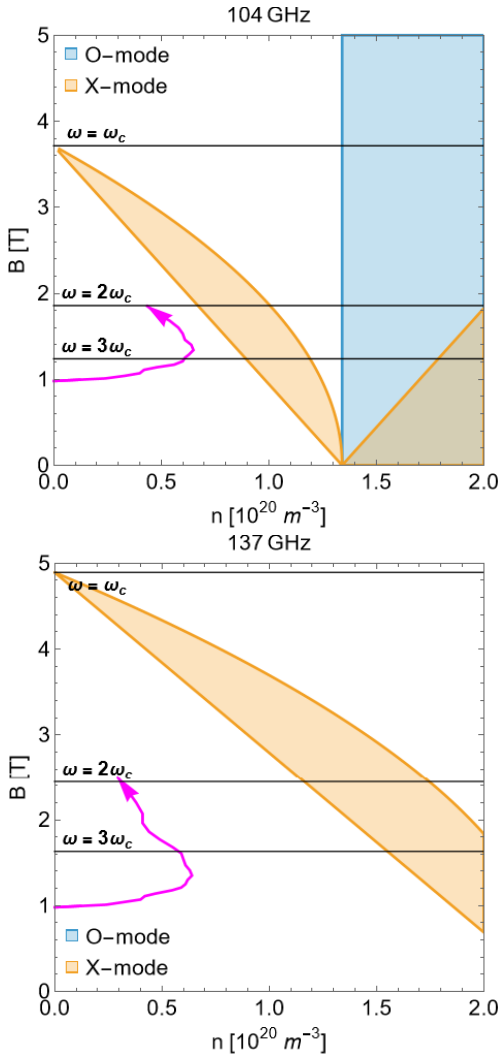


**Figure 2.** Accessibility of X- and O-mode at 104 and 137 GHz. Non-propagating regions are shaded in the respective colors. For illustration, the ray trajectories of Fig. 3 and Fig. 4 are reproduced (magenta) in the respective accessibility diagram.

## 3 Time-dependent modelling results

### 3.1 Prototypical ST40 discharge

First, let us consider the addition of 1 MW ECRH to a prototypical ST40 discharge. Notably, this shot (# 11336) features 1 MW of NBI and has $B$(40 cm) = 1.8 T; more details can be found in Refs. [8, 9]. The TRANSP simulations use the TGLF transport model without a sawtooth model for the core region, but including the scrape-off layer box model [9–11] for more accurate separatrix boundary conditions. For all simulations, the density profile is prescribed to match the experimental measurements while the temperature and current density profiles are predicted (even for the case of no applied ECRH).

The EC propagation and absorption is modeled as a single ray using the GENRAY code [12]. For a launcher located at $z$ = 9 cm above midplane and $R$ = 102.6 cm with angular aiming range ($\pm 10°, \pm 20°$) (poloidally and toroidally, respectively), we choose to inject the 104 GHz EC ray at $(-9°, 5°)$ and the 137 GHz EC ray at $(-8°, 13°)$. As shown in Figs. 3 and 4, these choices are made due to the relatively high density and low field of ST40 for these frequencies: 104 GHz must be injected nearly perpendicularly to minimize refraction (Fig. 2), while 137 GHz must be injected nearly parallel to enable a second pass through the resonance to increase absorption (Fig. 1) before encountering the plasma boundary. As such, there is little freedom to shape the resulting EC current drive profile.

The results of time-dependent modeling with TRANSP for both frequencies are shown in Figs. 5 - 7. First of all, it is clear that the power absorbed at 137 GHz (around 500 kW) is insufficient to modify the plasma behavior. This is largely because the absorption is out in the edge of the plasma where transport is high. It should be noted that these simulations do not contain a pedestal model, so it might be possible that the edge heating could raise the pedestal temperature and improve the X2

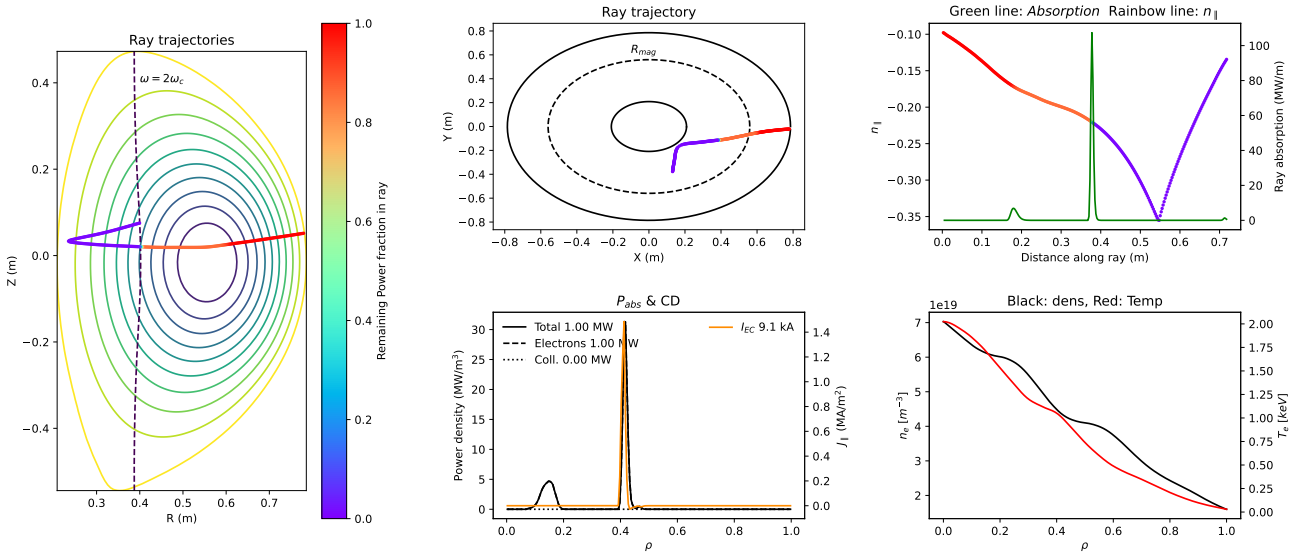


**Figure 3.** Ray trajectories and other relevant information for 104 GHz X2-mode ECRH on ST40 shot 11336 at 90 ms.

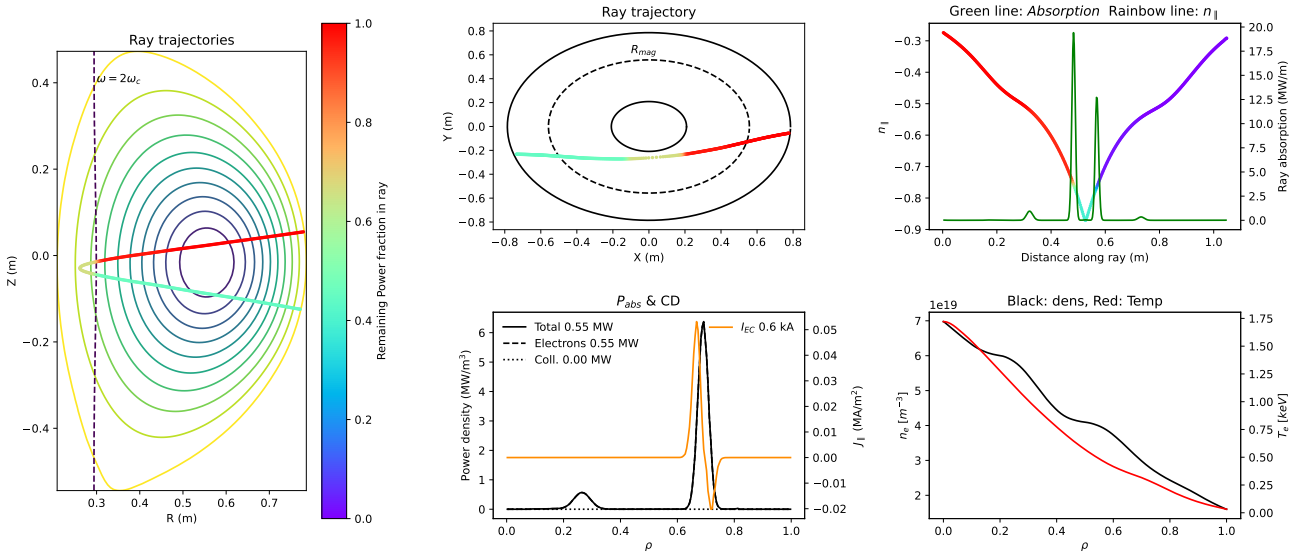


**Figure 4.** Same as Fig. 3 but for 137 GHz.

absorption at 137 GHz as time progresses, but this would need to be confirmed with additional simulations.[1]

In contrast, X2 ECRH at 104 GHz is seen to result in about a 33% increase in central temperature (from ~1.5 keV to ~2 keV) and a 33% decrease in the loop voltage (from ~1.5 V to ~1 V). The decrease in loop voltage is due to both the current directly driven by the EC (a few kA) and the increased bootstrap current indirectly driven by the EC via the increased central electron temperature. Non-inductively driving current via simply heating the plasma in this manner features prominently in rampup schemes proposed for ST-based fusion pilot plants [13]. The $q$ profile is seen to develop reversed shear near the center and raise above the $q = 1$ sawtooth threshold with the additional ECRH for much of the shot. This might enable ST40 to explore advanced operational scenarios relevant for fusion pilot plants (such as forming internal transport barriers, etc.). Including a sawtooth model into the simulations is needed to confirm this behavior, however.

Lastly, it is worth briefly noting that this shot (11336) exhibits strong transient behavior around 120 ms associated with a narrowing of the scrape-off layer and broadening of the core density profile [8, 9]. As a result, both frequencies experience significantly reduced absorption during this time period.

### 3.2 Ohmic ST40 discharge

Next, let us consider an alternative ST40 scenario in which there is no NBI, and only MC startup and solenoid

[1]Note that the poor performance of 137 GHz here and in the following scenario is not simply due to the reduced amount of absorbed power compared to 104 GHz; injecting 104 GHz at only 0.5 MW still results in visibly modified behavior compared to the baseline scenario.

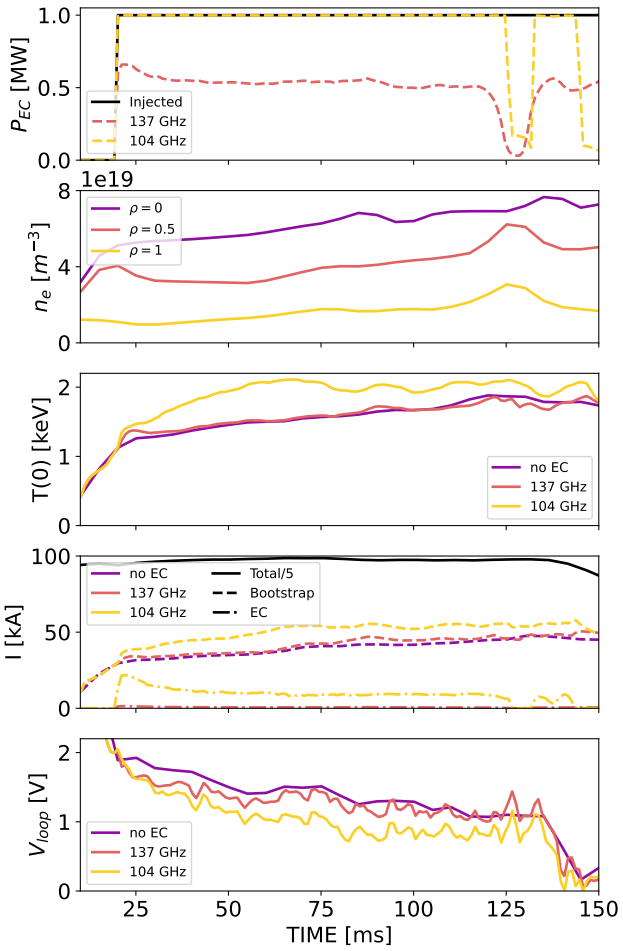


**Figure 5.** Time-evolution for the specified quantities with and without 1 MW X2-mode ECRH at either 104 or 137 GHz for the prototypical ST40 discharge provided by shot 11336. Importantly, note that the total plasma current $I_p \approx 500$ kA has been divided by five to fit on the figure axes.

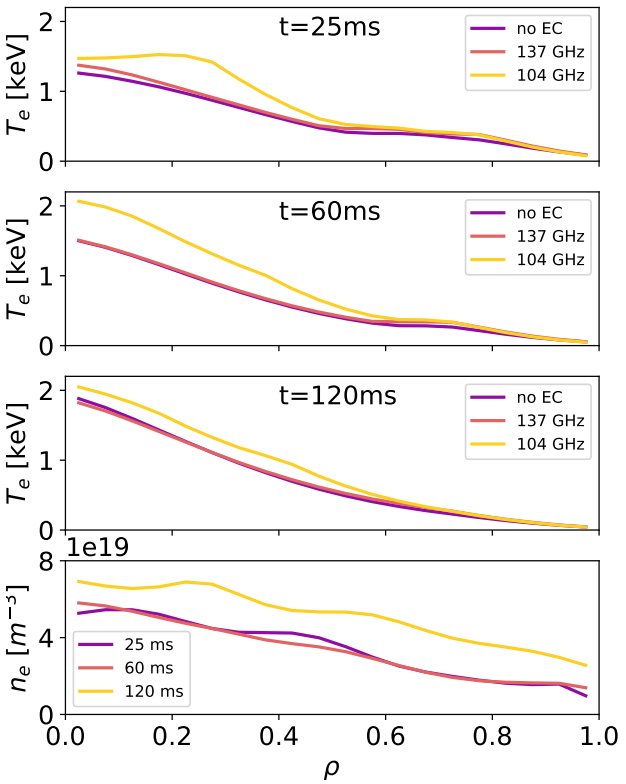


**Figure 6.** Temperature and density profiles at selected times with and without 1MW X2-mode ECRH at either 104 or 137 GHz for the prototypical ST40 discharge provided by shot 11336.

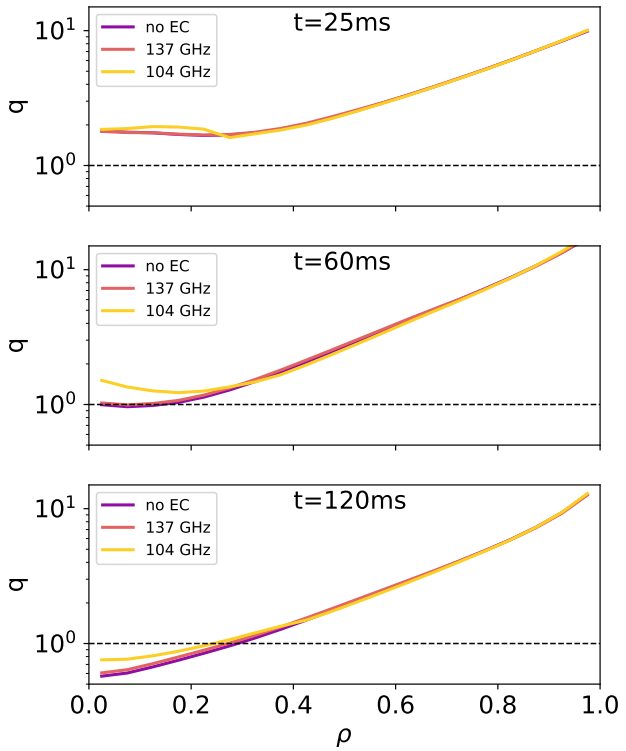


**Figure 7.** Same as Fig. 6 but for the $q$ profile.

sustainment are present (the so-called 'Ohmic' scenario on ST40). This scenario is particularly reactor-relevant for proposed EC-only devices because there is no NBI-provided rotation that can significantly alter plasma transport. The TRANSP simulations are based on the reference shot #11294, which has similar density and identical field $B(40\ \text{cm}) = 1.8$ T as the previous scenario (shot 11336). Consequently, the 104 and 137 GHz rays experience the same constraints as in the previous scenario (low accessibility versus low absorption); the 104 and 137 GHz rays are correspondingly launched at angles $(-5°, 5°)$ and $(-5°, 13°)$, respectively. The ray propagation is qualitatively similar to that shown in Figs 3 and 4, and will not be shown for brevity. The electron transport model is the same as for the previous scenario (TGLF), but now the ion transport is reduced to neoclassical levels to better reproduce the experimental measurements.

The time-evolution of select plasma parameters in response to the 104 and 137 GHz ECRH is shown in Figs. 8 - 10. Similar to the previous scenario, the 137 GHz ECRH does not significantly modify the plasma behavior even though 500 kW of microwave power is absorbed. The im-

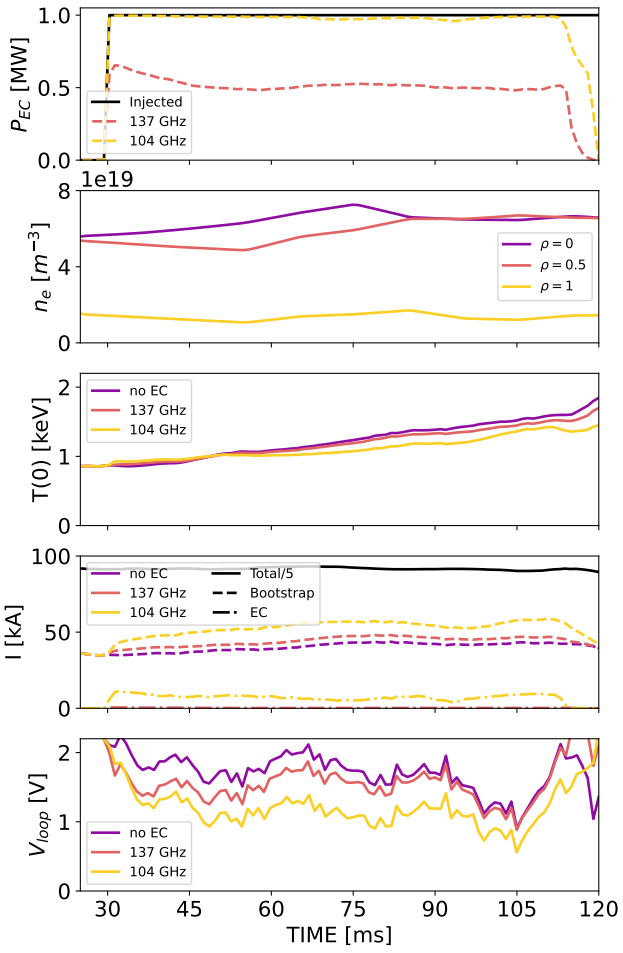


**Figure 8.** Same as Fig. 5 but for an Ohmic ST40 discharge provided by shot 11294.

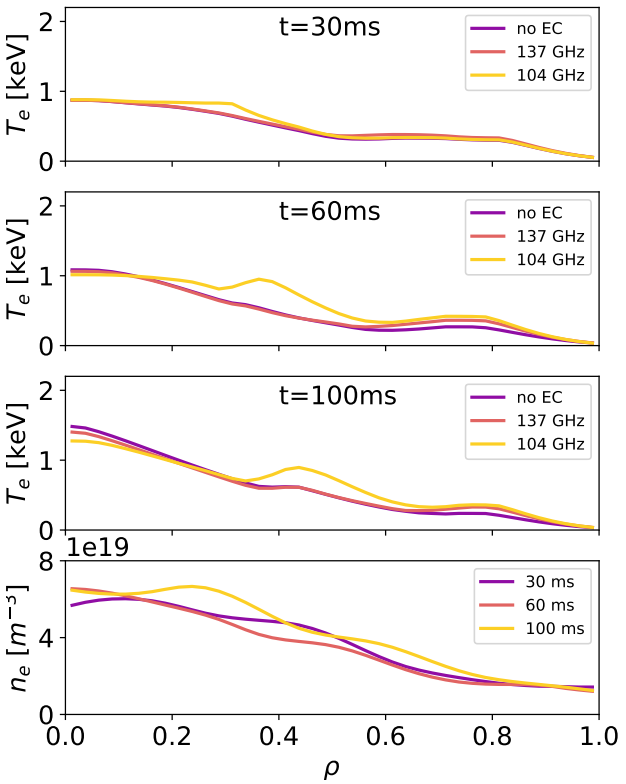


**Figure 9.** Same as Fig. 6 but for an Ohmic ST40 discharge provided by shot 11294.

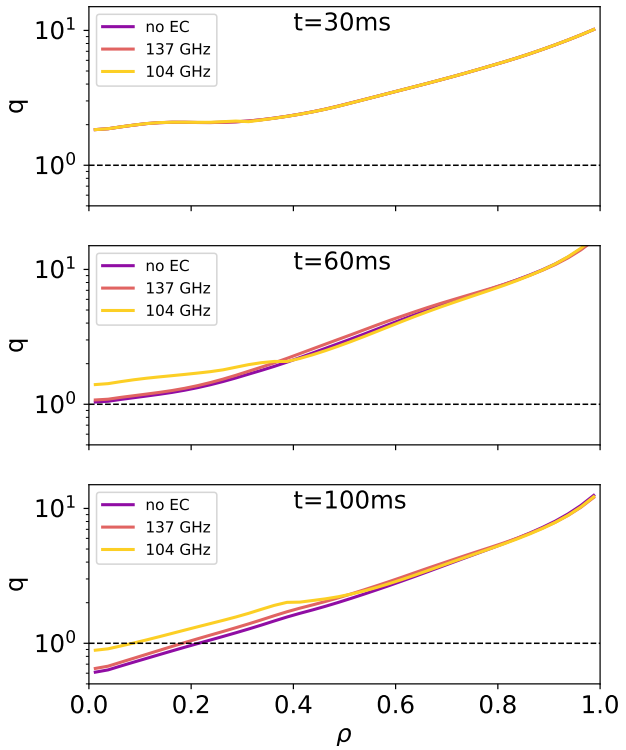


**Figure 10.** Same as Fig. 7 but for an Ohmic ST40 discharge provided by shot 11294.

pact for this scenario is slightly better than the previous scenario, however, as can be seen by the minor increase in bootstrap current and corresponding decrease in loop voltage when comparing the 137 GHz and no-EC cases in Fig. 8 that are absent from Fig. 5.

Like the previous scenario, the 104 GHz ECRH is able to visibly modify the plasma evolution. The loop voltage is seen to decrease by a similar factor of ~33% by a combination of directly driven EC current and increased bootstrap current from electron heating. In this case, however, the on-axis temperature profile is not increased; rather, as seen in Fig. 9, the ECRH increases the temperature off-axis at the resonance location and causes the temperature profile to become hollow at early times. In other words, the heating does not diffuse into the core for this scenario as it did in the previous one. This is likely due to the flattening of the $q$ profile [14] at the resonance location $\rho \sim 0.4$ observed in Fig. 10, although the flattened $n_e$ profile might also contribute. Again, the EC is able to raise the central $q$ value above $q = 1$ for a large fraction of the shot duration, although unlike the previous scenario no reversed-shear profile is achieved in the core region.

## 4 Beam-tracing results

We also performed time-dependent beam-tracing simulations using TORBEAM [15] within TRANSP for both frequencies to confirm the ray-tracing predictions obtained above using only a single ray to represent the EC beam. The same launcher position and injection angle were used, but beam-tracing also requires initial conditions for the injected beam waist $W$ and phasefront radius of curvature $R$; these were set to be $W = 4.174$ cm, $R = 122.3$ cm and $W = 3.437$ cm, $R = 172.7$ cm for 104 and 137 GHz, respectively. The values for $W$ are obtained assuming free-space paraxial propagation of a Gaussian beam with an initial waist of 2.043 cm over a distance of 81 cm from the waveguide exit to the focusing mirrors, while the values for $R$ are such that the beams re-focus at nominal distance of 86.5 cm in free space.

The results of using beam-tracing are nearly identical to the ray-tracing results presented in Figs 5-10. The only noticable difference is that TORBEAM predicts a smaller EC-driven current than GENRAY, but this is inconsequential since the two scenarios do not depend on ECCD. The power deposition profile is also slightly broader for beam-tracing, but this did not lead to any differences in the resulting temperature profiles.

## 5 Conclusion

In this work we perform time-dependent modeling of 104/137 GHz X2-mode ECRH on ST40 using the transport code TRANSP, in preparation for dedicated experiments utilizing the newly delivered 1 MW gyrotron from Kyoto Fusioneering. It is seen that for standard ST40 operating parameters (on-axis field ~1.8 T, central densities $\sim 7\times10^{19}$ m$^{-3}$) both frequencies have strong constraints on the launcher geometry for effective ECRH: for 104 GHz the accessibility is marginal (central density is approaching the X-mode cutoff density) so the launcher must be oriented to inject waves with small toroidal angles to minimize refraction away from the resonance. Conversely, for 137 GHz the resonance is located far from the plasma core ($\rho \gtrsim 0.6$) where the plasma is cold and the absorption is correspondingly weak, so the launcher must be oriented to inject waves with large toroidal angles to avoid intersecting the centerstack and instead traverse the resonance layer twice before exiting the plasma, thereby maximizing the absorption length. Both these constraints mean that there is little freedom to further tailor the desired current drive profiles.

Nevertheless, for two distinct ST40 scenarios at 1.8 T, we show that 104 GHz ECRH is able to reduce the loop voltage by ~33% through a combination of direct EC current drive and increased bootstrap current resulting from the EC heating. Since the ST40 solenoid is used primarily for flattop sustainment (with breakdown to full current provided by MC startup), this reduction in loop voltage may be directly translated into a comparable increase in the ST40 flattop duration. This will expand the variety of physics scenarios that can be explored on ST40 during the next experimental campaign. Also, the ECRH is seen to be able to raise the central $q$ value above unity for both scenarios, with locally flattened and reversed-shear $q$ profiles being possibly obtained. Since $q$-profile tailoring is expected to play a significant role in future reactor designs and operations, this result may allow ST40 to explore such advanced scenarios.

The next steps to be undertaken in this modelling effort are to (1) include a sawtooth model for more accurate $T_e(0)$ predictions, (2) explore alternate transport models that would allow the impact of internal transport barriers formed from non-monotonic $q$ profiles to be accurately assessed [16], and (3) consider reference plasmas at higher toroidal fields, or artificially re-scale the plasma field for these existing reference plasmas. This final step is because it is planned to increase the ST40 magnetic field to 2.4 T during the EC experimental campaign; as a result, the absorption constraints on the 137 GHz EC will be removed (resonance moving into the hotter plasma core), yielding increased experimental flexibility with regards to the EC injection angles. We can summarize our results in a final recommendation: since adding the new gyrotron to standard ST40 scenarios appears to result in only modest improvements, efforts should now be devoted towards designing entirely new scenarios for ST40 that will maximize the impact of the extra ECRH power.

## References

[1] E. Tholerus et al., Flat-top plasma operational space of the step power plant, Nucl. Fusion **64**, 106030 (2024). https://doi.org/10.1088/1741-4326/ad6ea2

[2] A. Alieva et al., 25th Topical Conference on Radio-Frequency Power in Plasmas, Schloss Hohenkammer, Germany, May 19-22 (2025).

[3] S.A.M. McNamara et al., Overview of recent results from the ST40 compact high-field spherical tokamak, Nucl. Fusion **64**, 112020 (2024). https://doi.org/10.1088/1741-4326/ad6ba7

[4] E.J. du Toit, V.F. Shevchenko, Development of an electron cyclotron resonance heating and electron bernstein wave current drive system on ST40, Plasma Phys. Control. Fusion **64**, 115015 (2022). https://doi.org/10.1088/1361-6587/ac97bf

[5] N.A. Lopez, F.M. Poli, Regarding the optimization of O1-mode ECRH and the feasibility of EBW startup on NSTX-U, Plasma Phys. Control. Fusion **60**, 065007 (2018). https://doi.org/10.1088/1361-6587/aabaa8

[6] A.Y. Pankin et al., TRANSP integrated modeling code for interpretive and predictive analysis of tokamak plasmas, Comput. Phys. Commun. **312**, 109611 (2025). https://doi.org/10.1016/j.cpc.2025.109611

[7] R. Prater, Heating and current drive by electron cyclotron waves, Phys. Plasmas **11**, 2349 (2004). https://doi.org/10.1063/1.1690762

[8] X. Zhang et al., Experimental observations of bifurcated power decay lengths in the near scrape-off layer of ST40 High Field Spherical Toka-

mak, Nucl. Mater. Energy **41**, 101772 (2024). https://doi.org/10.1016/j.nme.2024.101772

[9] X. Zhang et al., Core-edge integrated predictive studies of ST40 and NSTX plasmas with the scrape-off layer box model, Phys. Plasmas **32**, 032513 (2025). https://doi.org/10.1063/5.0251145

[10] X. Zhang et al., Reduced physics model of the tokamak scrape-off-layer for pulse design, Nucl. Mater. Energy **34**, 101354 (2023). https://doi.org/10.1016/j.nme.2022.101354

[11] M.S. Anastopoulos Tzanis et al., Integrated modeling of ST40 hot ion plasmas using the TGLF transport model, Plasma Phys. Control. Fusion **67**, 055022 (2025). https://doi.org/10.1088/1361-6587/adce2f

[12] A.P. Smirnov, R.W. Harvey, The GENRAY ray tracing code, Report CompX-2000-01 (2003).

[13] Y. Takase et al., 25th Topical Conference on Radio-Frequency Power in Plasmas, Schloss Hohenkammer, Germany, May 19-22 (2025). https://www.ipp.mpg.de/5533603

[14] G. Vlad et al., A general empirically based microinstability transport model, Nucl. Fusion **38**, 557 (1998). https://doi.org/10.1088/0029-5515/38/4/307

[15] E. Poli et al., TORBEAM 2.0, a paraxial beam tracing code for electron-cyclotron beams in fusion plasmas for extended physics applications, Comput. Phys. Commun. **225**, 36 (2018). https://doi.org/10.1016/j.cpc.2017.12.018

[16] F.M. Poli et al., External heating and current drive source requirements towards steady-state operation in iter, Nucl. Fusion **54**, 073007 (2014). https://doi.org/10.1088/0029-5515/54/7/073007